Journal of Food Safety and Food Quality
Archiv für Lebensmittelhygiene

J. Food Saf. Food Qual. **2025**; 76(4): 42752
https://doi.org/10.31083/JFSFQ42752

Original Research

Rapid Detection of Deoxynivalenol in Cereals Based on Amplified Luminescence Proximity Homogeneous Detection Technology

Dian Li[1,†], Jie Chen[2,†], Shangbin Kao[1], Canlong Yan[1], Tianyu Zheng[1], Yuan Qin[1], Xiumei Zhou[1], Nenghua Zhang[3], Biao Huang[1,*]

[1]College of Life Sciences and Medicine, Zhejiang Sci-Tech University, 310018 Hangzhou, Zhejiang, China
[2]Changshu Medicine Examination Institute, Changshu Municipal Health Commission, 215500 Suzhou, Jiangsu, China
[3]Jiaxing Hospital of Traditional Chinese Medicine, Zhejiang Chinese Medical University, 314001 Jiaxing, Zhejiang, China
*Correspondence: jswxhb@163.com (Biao Huang)
[†]These authors contributed equally.
Academic Editor: Corinna Kehrenberg
Submitted: 29 May 2025 Revised: 31 July 2025 Accepted: 11 August 2025 Published: 24 October 2025

Abstract

Background: To address challenges of low sensitivity, complex operation, and matrix interference in detecting deoxynivalenol (DON) in cereals, this study developed a novel wash-free detection system using amplified luminescence proximity homogeneous assay (AlphaLICA) technology. **Methods**: The method leverages energy transfer between microspheres and antigen-antibody interactions: DON antibodies competitively bind to DON-BSA-luminescent microspheres and DON standards/samples, with bound antibodies detected via goat anti-mouse IgG-conjugated photosensitive microspheres. **Results**: Results demonstrated a detection limit (LOD) of 1.03 ng/mL and quantitation limit (LOQ) of 7.57 ng/mL. Intra-/inter-batch coefficients of variation were $<$6.13% and 6.67%, respectively. Recovery rates in wheat, corn, and rice reached 97.52%–105.83% (relative standard deviation (RSD) $\leq$12.83%), with $<$0.21% cross-reactivity to aflatoxin B1. Compared to enzyme-linked immunosorbent assay (ELISA), AlphaLICA showed superior sensitivity (1.03 vs. 10 ng/mL), faster detection (5 vs. 35 min), broader linear range (7.57–800 vs. 12.5–200 ng/mL), and lower variability (6.13%/6.67% vs. 8%/12%). Pearson correlation analysis confirmed a strong association with ELISA results ($p < 0.001$, r = 0.8374). **Conclusions**: The established DON-AlphaLICA method provides a simple, rapid, sensitive, and accurate solution for DON detection, effectively addressing current limitations in grain safety monitoring. This innovative method enables efficient screening of mycotoxin contamination in agricultural products while minimizing procedural complexity.

Keywords: deoxynivalenol; wash-free detection; singlet oxygen; cereals; fast detection

1. Introduction

In the context of global climate change and high-density agricultural cultivation, mycotoxins are threatening human health in the form of food mildew [1–3]. As one of the secondary metabolites of Fusarium, deoxynivalenol (DON) has the characteristics of wide pollution range, complex toxicity mechanism and difficult prevention and control [4–6]. More seriously, DON not only causes acute gastroenteritis symptoms by inhibiting the activity of eukaryotic ribosomal peptidyl transferase, but also its chronic exposure is closely related to intestinal flora imbalance, immune tolerance imbalance and even cancer risk [7–9]. Studies have shown that DON can also induce pyroptosis of intestinal epithelial cells by activating the MAPK/NF-κB signaling pathway, which makes it clearer to understand its toxic mechanism [10,11]. Although the European Union, the United States and other countries have established a full chain supervision system from farmland to table, with advanced detection technologies such as High-Performance Liquid Chromatography-Mass Spectrometry (HPLC-MS) widely adopted in the EU for official monitoring of DON [12]. The food safety problems of cereals still occur frequently in developing countries due to the lag of detection technology [13,14]. As an illustration, the European Union regulates DON in maize-derived products and grains to a maximum threshold of 750 µg/kg, while China's GB2761-2011 mandates a DON limit of 1000 µg/kg for processed grains (e.g., maize, barley, wheat flours, and related derivatives). This stringent regulatory divergence necessitates detection methodologies with enhanced sensitivity and analytical precision to meet compliance standards.

The current DON detection methods are diverse, including immunoaffinity column-fluorescence detection (IAC-FLD), enzyme-linked immunosorbent assay (ELISA), colloidal gold immunochromatography and other methods [15–18]. Among them, the IAC-FLD method has higher requirements for experimental operation and instrument use and longer detection time [19,20]. In the ELISA method, the samples were processed and diluted according to the method in the kit, and the standard concentration of DON positive limit was 250 ng/mL. However, compared with the amplified luminescence proximity homogeneous assay (AlphaLICA) method, the standard curve range of the enzyme immunoassay kit (12.5–200 ng/mL vs. 7.57–800

ng/mL) was lower, which could not meet the detection of high concentration samples [21]. Colloidal gold rapid detection card is a commonly used rapid detection method, which can be used for the screening of a large number of samples. It has the advantages of relatively simple operation and rapid detection [22–24]. However, colloidal gold assays are limited to qualitative/semi-quantitative detection with compromised sensitivity and accuracy. Empirical data reveal 16% false-positive and 5% false-negative rates in wheat at critical DON thresholds, attributable to antibody cross-reactivity and subjective visual interpretation. These fundamental constraints prevent reliable rapid DON screening [23,25–27].

In this context, AlphaLICA technology has attracted academic attention due to its unique 'wash-free' design concept [28]. The technology activates the chemiluminescence substrate in the luminescent microsphere by the singlet oxygen generated by the laser excitation of the photosensitizer in the photosensitive microsphere, forming a spatially confined energy transfer network. This non-contact signal amplification mechanism not only avoids the washing loss problem of traditional ELISA, but also realizes the physical suppression of background signal through the short-range diffusion characteristics of singlet oxygen (the radius of action is less than 200 nm), which provides a new solution for complex matrix detection [29,30]. The purpose of this study is to establish a new, rapid and accurate DON-AlphaLICA detection method, which is expected to make an important contribution to the detection of toxins in cereals.

2. Materials and Methods

2.1 Reagents and Instruments

Immunochemical components including DON-BSA (Cat. No. STD03925, Beosen Biotech, Wuxi, China) conjugate, analytical-grade DON standards (Cat. No. STD03932, Beosen Biotech), murine-derived anti-DON monoclonal antibodies (Cat. No. MCH04290, Beosen Biotech), and a commercial DON ELISA kit (Cat. No. MYT03396, Beosen Biotech) were procured from Beosen Biotech . Cross-reactivity validation reagents (aflatoxin B1) originated from the same supplier. Secondary antibodies (goat anti-mouse IgG) were acquired from Biotech Biotechnology (Cat. No. Ov02-02, Biotech Biotechnology, Luoyang, China), with AlphaLICA luminescent microspheres (Cat. No. 67500002, Weidu Biotech, Suzhou, China) and photosensitive microspheres (Cat. No. 67700001, Weidu Biotech) obtained from Weidu Biotech. Biochemical reagents comprised Tris-base (Cat. No. V33729, Yuanye Biotech, Shanghai, China) and MES buffer (Cat. No. R21353, Yuanye Biotech), while Bovine Serum Albumin (BSA) (Cat. No. V900933, Sigma-Aldrich, Missouri, USA), Proclin 300 (Cat. No. 48918-U, Sigma-Aldrich) preservative, 1-Ethyl-3-(3-dimethylaminopropyl) carbodiimide (EDC) (Cat. No. 39391, Sigma-Aldrich) and N-Hydroxysuccinimide (NHS) (Cat. No. 130672, Sigma-Aldrich) were supplied by Sigma-Aldrich (Cat. No. V900933, Sigma-Aldrich). Methanol of high-performance liquid chromatography (HPLC) grade was sourced from Sinopharm Chemical (Cat. No. 40064260, Sinopharm Chemical, Shanghai, China) and microsphere stabilization solution from Boshi Biotech (Cat. No. B07258, Boshi Biotech,Hangzhou, China). In-house formulated buffers included: (1) blocking buffer (0.6% Tris-base, 0.2% BSA, 0.9% NaCl, 0.05% Proclin 300), (2) 2-(N-Morpholino) ethanesulfonic acid (MES)-based conjugation buffer (50 mM, pH 6.0), and (3) standard matrix (2.5 mM Tris-HCl with 0.5% BSA).

Experimental instrumentation encompassed a Suntad ultrasonic cleaner (Cat. No. E0434, Beyotime Biotechnology, Shanghai, China), Sigma-Aldrich 96-well immunoreaction plates (Cat. No. CLS2485, Sigma-Aldrich, Missouri, USA), and a thermostatic microplate shaker (Cat. No.170803, Kangjian Medical, Jiangsu, China). Fluorescence quantification was performed using an AlphaLICA signal detector (Cat. No. B8B23, Biotecs Intelligent Technology, Zhejiang, China).

2.2 Functional Modification of Microspheres

2.2.1 Luminescent Microspheres Coupled With DON-BSA

2.2.1.1 Washing of microspheres. 1 mg of Luminescent microspheres were dispensed into a 1.5 mL centrifugation tube, supplemented with 300 µL 50 mM MES buffer (pH 6.0), spun at 13,000 rpm for 20 min, and the supernatant was removed; MES buffer was applied for two additional rinses (200 µL per cycle), and the microspheres were reconstituted to a final concentration of 5 mg/mL using 200 µL MES buffer.

2.2.1.2 Carboxyl activation. A 1:2 molar ratio of EDC/NHS (5 µL of 20 mg/mL EDC: 10 µL of 20 mg/mL NHS) was added sequentially to purified microspheres. The mixture was vortex-mixed and incubated at 37 °C for 20 min in the dark. After centrifugation at 13,000 rpm for 20 min, the supernatant was discarded, and the pellet was reconstituted in 400 µL tagging buffer, sonicated for 30 sec, and washed twice with phosphate-buffered saline (PBS).

2.2.1.3 Antigen coupling. 0.1 mg DON-BSA was mixed with activated microspheres and incubated at 37 °C for 2 h. After centrifugation at 13,000 rpm for 20 min, the supernatant was discarded, 800 µL of blocking buffer was added, and blocked at 37 °C for 1 h in the dark.

2.2.1.4 Product preservation. After centrifugation, the supernatant was discarded, ultrasonically dispersed with 1 mL blocking buffer, and repeatedly washed twice. Finally, the microspheres were resuspended with 500 µL microsphere preservation solution to a final concentration of 2 mg/mL,

and stored at 4 °C in dark. The coupling amount of carboxyl microspheres was 119.8 mg/g.

2.2.2 Photosensitive Microspheres Coupled With Goat Anti-mouse IgG

2.2.2.1 Microspheres pretreatment. 1 mg photosensitive microspheres were taken, and MES buffer was washed and the concentration was adjusted according to the above 2.2.1 steps (final concentration 5 mg/mL).

2.2.2.2 Antibody coupling. 0.1 mg goat anti-mouse IgG was combined with functionalized microspheres, maintained at 37 °C for 2 h under light protection, and spun at 13,000 rpm for 20 min to eliminate the liquid phase.

2.2.2.3 Aldehyde reduction. 10 µL of 1 mol/L $NaBH_4$ (formulated using ultrapure water) was supplemented and maintained at 37 °C under light-protected conditions for two hours.

2.2.2.4 Closure and purification. After centrifugation, the liquid phase was removed and passivated with 800 µL blocking buffer for 1 hour (under light-protected conditions at 37 °C), succeeded by sonicated homogenization with 600 µL blocking buffer, duplicate washing cycles, and ultimately reconstituted with 500 µL microsphere preservation solution to a particle density of 2 mg/mL, preserved in a light-protected environment at 4 °C.

2.3 Optimization of Detection System

To enhance the analytical performance, systematic optimization was performed on three critical parameters: the mixing ratio between photosensitive microspheres and Luminescent microspheres, antibody (DON-Ab) concentration, and incubation duration during immunoreaction. With a lower half-maximal inhibitory concentration (IC_{50}) value and a higher F_{max}/IC_{50} value as the selection criteria, the larger the F_{max}/IC_{50} value, indicating that the detection system has high signal output capacity (high F_{max}) and high sensitivity (low IC_{50}). At the same time, in order to obtain higher sensitivity, the sample addition method was also optimized. Due to the dilution coefficient K = 20, the final matrix concentration was 1 ng/mL = 20 µg/kg.

2.4 Method Evaluation

2.4.1 Precision

An identical criterion was employed for 10 replicate analyses, and the intra-assay variability metric (CV) was assessed by deriving the mean concentration and standard deviation. Concurrently, the inter-batch variability metric was quantified through three separate experimental trials. The coefficient of variation (CV) served as the precision assessment parameter, with the computational expression defined as: CV (%) = (standard deviation/mean) × 100.

2.4.2 Sensitivity

The analytical detectability of the assay was defined as the limit of detection (LOD) in this investigation. The averaged mean blank signal value (F) and its associated variability (SD) were quantified through 10 replicated assays of negative controls (analyte-free conditions). The LOD and limit of quantitation (LOQ) were established following Eurachem criteria: LOD represented the analyte level equivalent to the blank signal magnitude reduced by threefold SD (F-3SD), whereas LOQ corresponded to F-10SD, as validated against the calibration curve [31].

2.4.3 Specificity

Under the optimal reaction conditions, the cross-reaction rate was determined with aflatoxin B1 (AFB1) as the interfering substance. The calculation formula of cross-reaction rate is: cross-reaction rate = actual concentration/theoretical concentration × 100%.

2.4.4 Recovery Rate

The standard addition method was used to evaluate the recovery rate: the DON standard solution with known concentration was added to the fully homogenized blank grain sample at a ratio of 1:9 to prepare the spiked sample (n = 9). After the sample was pretreated, the total DON concentration was detected by AlphaLICA method in this experiment. After deducting the background value of the blank sample without standard addition, the recovery rate was calculated according to the following formula: Recovery = (C measured – C blank)/C spiked × 100% (C measured is the mean value of the detected concentration of the spiked sample, C blank is the background concentration of the blank sample, and C spiked is the theoretical concentration of the added standard solution).

2.5 Sample Handling

Weigh 5.0 g grain samples (Note: crushed, sieved through 20 mesh) in a 100 mL stopper triangle bottle, accurately add 25 mL 10% methanol water (1:9) solution, close, shake for 10 min (200 rpm), take the appropriate amount of methanol water extract of the sample in a centrifuge tube, more than 3500 rpm, centrifuge for more than 5 min, take the intermediate layer of the supernatant, that is, the sample extract. Take 0.2 mL sample extract, add 0.6 mL standard working solution, and mix well to obtain the sample solution to be tested (dilution coefficient K = 20). The sample solution to be tested was analyzed by AlphaLICA.

2.6 ELISA Detection Scheme of DON

The DON levels in the test material were quantified via ELISA (Beosen Biotech, Cat. No. MYT03396, Wuxi, China) to validate the analytical robustness of the AlphaLICA assay. The pre-coated microplates were sequentially added with 0, 12.5, 25, 50, 100, 200 ng/mL DON standard solution and the sample to be tested. Each well was added

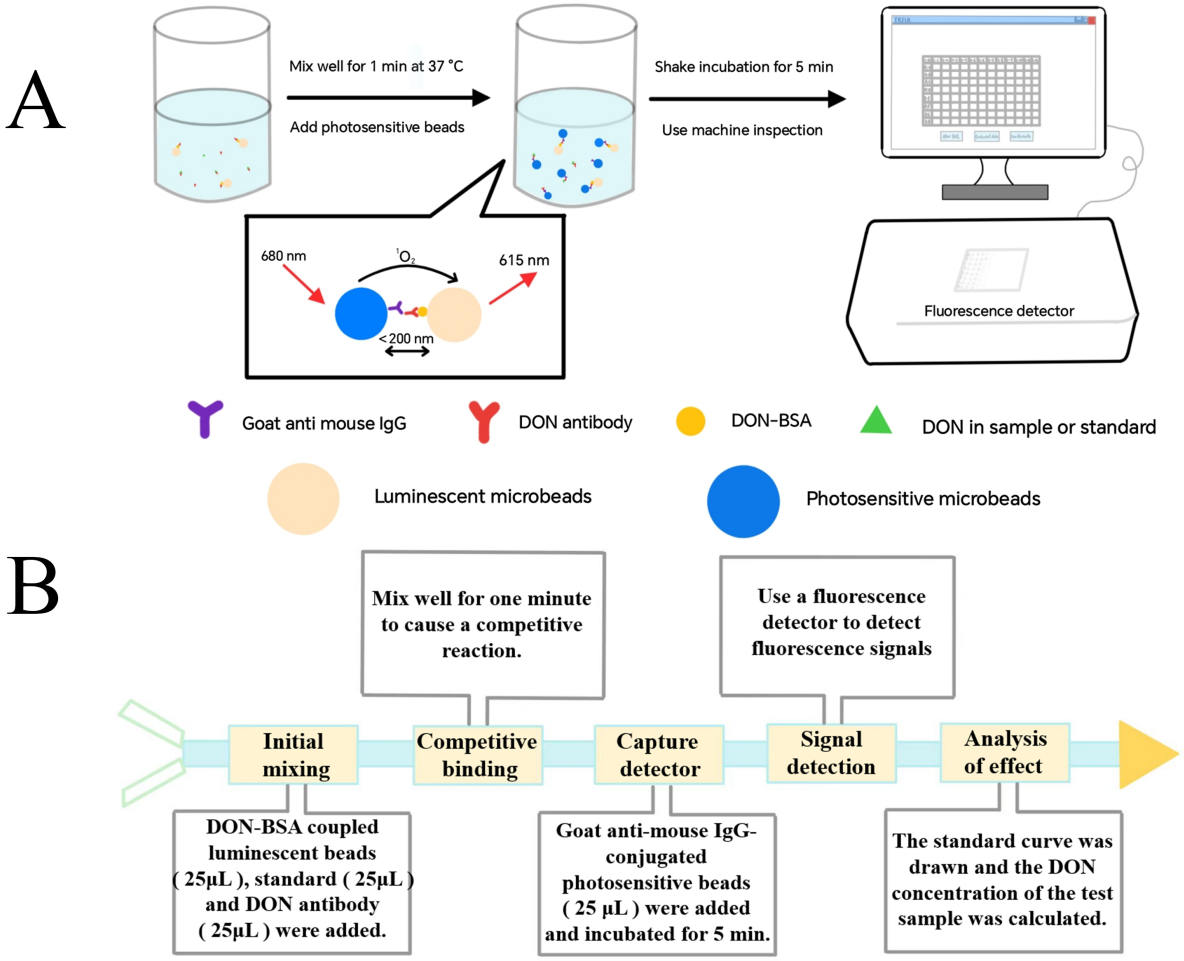

Fig. 1. Principle and Flowchart of AlphaLICA. (A) AlphaLICA System Schematic for DON detection. (B) Flowchart of DON-AlphaLICA. DON, Deoxynivalenol; BSA, Bovine Serum Albu-min.

with 50 µL DON antibody solution and 50 µL horseradish peroxidase (HRP) labeled secondary antibody solution, respectively. After incubation at 37 °C for 20 min, the reaction solution was discarded, and the micropores were washed four times with washing buffer. Subsequently, 50 µL chromogenic substrate (TMB) and 50 µL termination solution (2 mol/L H_2SO_4) were added to each well, and the chromogenic reaction was carried out at 37 °C for 15 min in the dark. The absorbance (OD value) was immediately determined at 450 nm wavelength. The Logit-log linear regression standard curve was established with the standard concentration (No.1–6 holes) as the abscissa and the Logit value of the corresponding OD value as the ordinate, and the DON concentration corresponding to the OD value of the sample hole was calculated.

2.7 Statistical Analysis

Data analysis was performed using SPSS Statistics 26 software (SPSS Inc., Chicago, IL, USA), specifically including: (1) assessing the strength of association between data obtained from ELISA and AlphaLICA technology; (2) calculating the half-maximal inhibitory concentration (IC_{50}) of AlphaLICA. First, the Shapiro-Wilk test was used to determine whether the data followed a normal distribution. Based on this, appropriate correlation analysis methods were selected: Pearson correlation analysis was used for data that followed a normal distribution, while Spearman rank correlation analysis was used for data that did not follow a normal distribution. The statistical significance level was set at $p < 0.05$.

3. Results

3.1 DON-AlphaLICA Detection Principle

In this study, a highly sensitive detection system for DON was constructed based on the principle of AlphaLICA determination (Fig. 1). The DON-BSA complex was covalently coupled to the surface of the luminescent microspheres by carbodiimide method (EDC/NHS), and the goat anti-mouse IgG was coupled to the surface of the photosensitive microspheres by reductive amination [32,33]. When the free DON in the sample competes with the DON-BSA on the luminescent microsphere to bind to the antibody, the

antibody binds to the goat anti-mouse IgG secondary antibody coupled to the photosensitive microsphere through the Fc segment, and the distance between the two microspheres is shortened to less than 200 nm. Under irradiation with a 680 nm laser, the generated singlet oxygen from the photosensitive microspheres transferred to the Luminescent microspheres, triggering the europium chelate to produce the distinct emission at 615 nm. The signal magnitude exhibited an inversely proportional relationship to the DON concentration in the test material [34].

3.2 Optimization of DON-AlphaLICA

In this study, based on the principle of minimizing the IC_{50} value of the dose-effect curve and maximizing the F_{max}/IC_{50} ratio, a single-factor rotation optimization strategy was used to systematically screen the key parameters of the DON-AlphaLICA system. By constructing a gradient of 0–800 ng/mL DON standard solution, the following optimization experiments were completed in turn.

3.2.1 Optimization of the Concentration of DON-BSA Coupled Luminescent Microspheres

The DON-BSA coupled luminescent microspheres were diluted by 1:50, 1:100, 1:200, 1:400, 1:800 gradient dilution, fixed antibody concentration (600 ng/mL) and photosensitive microspheres dilution ratio (1:50), reaction time 5 min. As shown in Fig. 2A, the 1:50 dilution group showed the best detection performance (IC_{50} = 20.3 ng/mL, F_{max}/IC_{50} = 3644.09). The results show that the high concentration of DON-BSA coupled luminescent microspheres can enhance the competitive reaction kinetics and improve the detection sensitivity.

3.2.2 Optimization of the Concentration of Goat Anti-mouse IgG-conjugated Photosensitive Microspheres

Based on the optimized conditions of luminescent microspheres at 1:50 and the fixed antibody concentration (600 ng/mL), the dilution effect of goat anti-mouse IgG coupled photosensitive microspheres was investigated, and diluted at 1:50, 1:100, 1:200, 1:400, and 1:800 gradients. As shown in Fig. 2B, the F_{max}/IC_{50} value of the 1:50 dilution ratio group (F_{max}/IC_{50} = 3911.2) was significantly higher than that of the other groups, and there was a lower IC_{50} value (IC_{50} = 20.8 ng/mL), confirming that high concentrations of goat anti-mouse IgG-conjugated photosensitive microspheres help to enhance the bridging efficiency and optimize the energy transfer path.

3.2.3 Antibody Working Concentration Screening

Under the 1:50 dilution system of double microspheres, the effects of antibody concentrations at 300 ng/mL, 600 ng/mL, 900 ng/mL, 1200 ng/mL and 1800 ng/mL on the detection performance were systematically evaluated. As shown in Fig. 2C, the 600 ng/mL antibody group showed the optimal equilibrium characteristics (IC_{50} = 21.14 ng/mL, F_{max}/IC_{50} = 1875.69), and the fluorescence base met the detection requirements. The Logit-log linear regression fitting degree (r = 0.99807) indicated that moderate antibody concentration could coordinate competitive binding and signal generation efficiency.

3.2.4 Screening of Reaction Time

On the basis of optimizing the parameters of microspheres and antibodies, the effects of reaction time on the detection performance were investigated according to the time gradient of 1 min, 5 min, 15 min and 25 min. As shown in Fig. 2D, the IC_{50} value (IC_{50} = 21.25 ng/mL) of the 5 min reaction group was lower than that of the other time groups, and the fluorescence base of F_{max}/IC_{50} (F_{max}/IC_{50} = 2202.49) met the experimental detection requirements, and the slope of the curve at this point was significantly higher than that of the other time groups, which had the ability to express the reaction results with high efficiency.

3.2.5 Validation of Sample Addition Method Optimization

Based on the above reaction conditions, the detection performance was screened by two sampling strategies: (1) Stepwise incubation method: DON-BSA-luminescent microspheres, standard/test samples and DON antibodies were added to the reaction wells in turn. After vortex mixing, goat anti-mouse IgG-conjugated photosensitive microspheres were added and the competitive signal was detected. (2) Synchronous incubation method: DON-BSA-luminescent microspheres, standard/test samples, DON antibody and goat anti-mouse IgG-conjugated photosensitive microspheres were added to the reaction well at one time, and reacted in the dark for 5 min before direct detection. As shown in Fig. 2E, the half inhibitory concentration (IC_{50} = 21.26 ng/mL) and signal response ratio (F_{max}/IC_{50} = 2511.95) of the step-by-step sampling group were significantly better than those of the synchronous sampling group, which confirmed that the sampling sequence affected the reaction kinetics of the detection system, and the step-by-step incubation strategy could effectively improve the antigen-antibody binding efficiency and detection sensitivity.

3.3 Methodological Evaluation of DON-AlphaLICA

In this study, the comprehensive performance of the DON-AlphaLICA detection system was verified by systematic evaluation. The standard curve constructed based on the optimized conditions, as shown in Fig. 3, Logit (Y) and DON concentration logarithm (lg [DON]) showed a significant linear correlation (Logit (Y) = 2.83129 – 2.16282 × X, r = 0.99726), where Y = F/F0 (sample to blank fluorescence intensity ratio), X = lg [DON concentration (ng/mL)]. The analytical detectability of the assay exhibited a broad calibration span of 7.57–800 ng/mL, demonstrated an IC_{50} value of 20.47 ng/mL, and achieved detectability thresholds (LOD and LOQ) of 1.03 ng/mL and 7.57 ng/mL, respectively. The precision analysis showed that the intra-

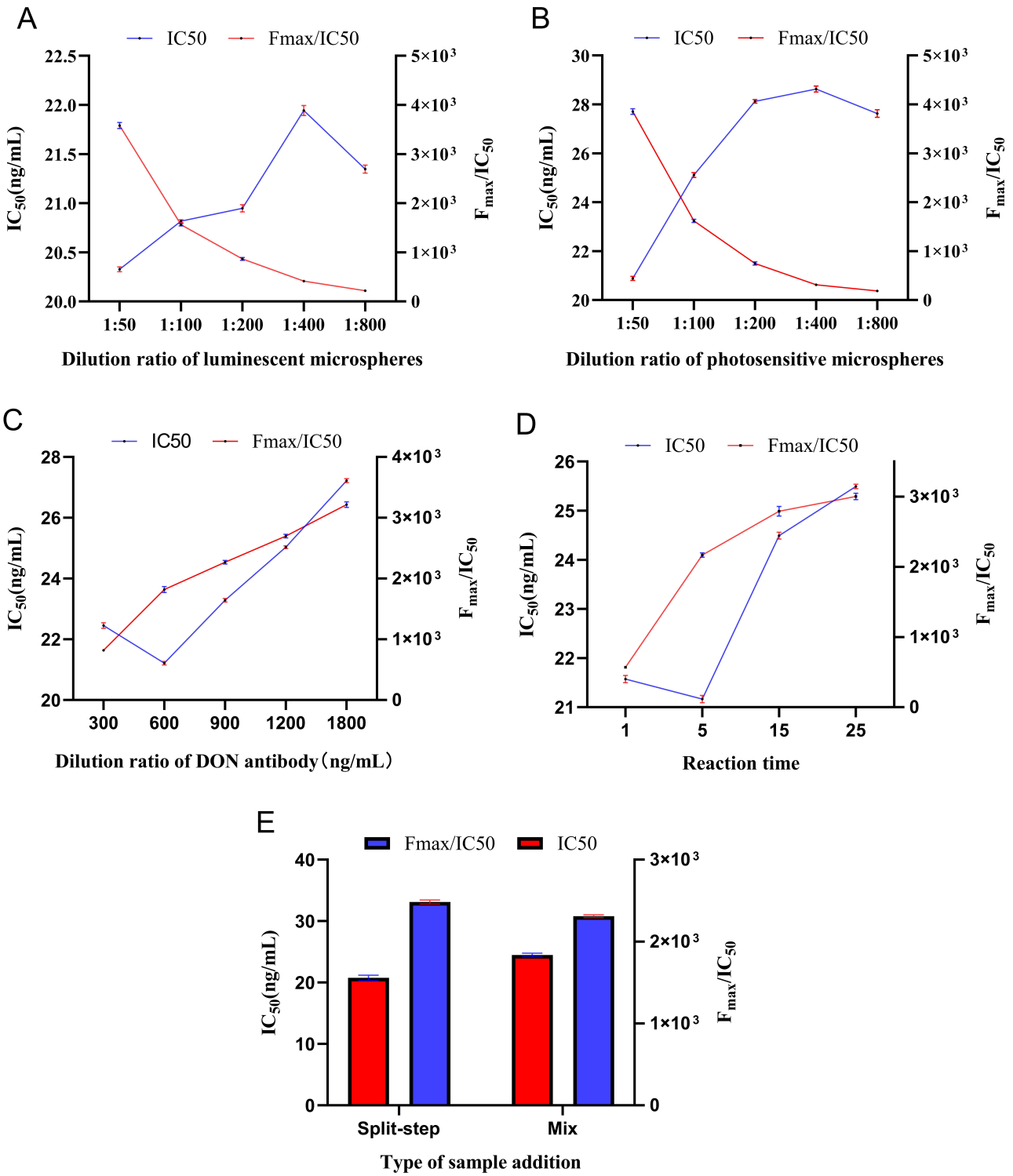

Fig. 2. DON-AlphaLICA optimization conditions. (A) F_{max}/half-maximal inhibitory concentration (IC_{50}) and IC_{50} values of DON-BSA coupled luminescent microspheres at 1:50, 1:100, 1:200, 1:400 and 1:800 dilution ratios. (B) F_{max}/IC_{50} and IC_{50} values of goat anti-mouse IgG-conjugated photosensitive microspheres at 1:50, 1:100, 1:200, 1:400 and 1:800 dilution ratios. (C) F_{max}/IC_{50} and IC_{50} values at antibody concentrations of 300, 600, 900, 1200, and 1800 ng/mL. (D) F_{max}/IC_{50} and IC_{50} values at 1, 5, 15, 25 min reaction time. (E) F_{max}/IC_{50} and IC_{50} values under two sampling methods: step-by-step incubation method and synchronous incubation method.

assay ($n_1 = 10$) and inter-assay ($n_2 = 3$) coefficients of variation were 4.48%–6.13% and 3.68%–6.67%, respectively, as shown in Table 1, showing excellent repeatability. In the specificity verification, the cross-reaction rate of aflatoxin B1 was lower than 0.21% (threshold <1%), which confirmed that the antibody was highly specific. The accuracy

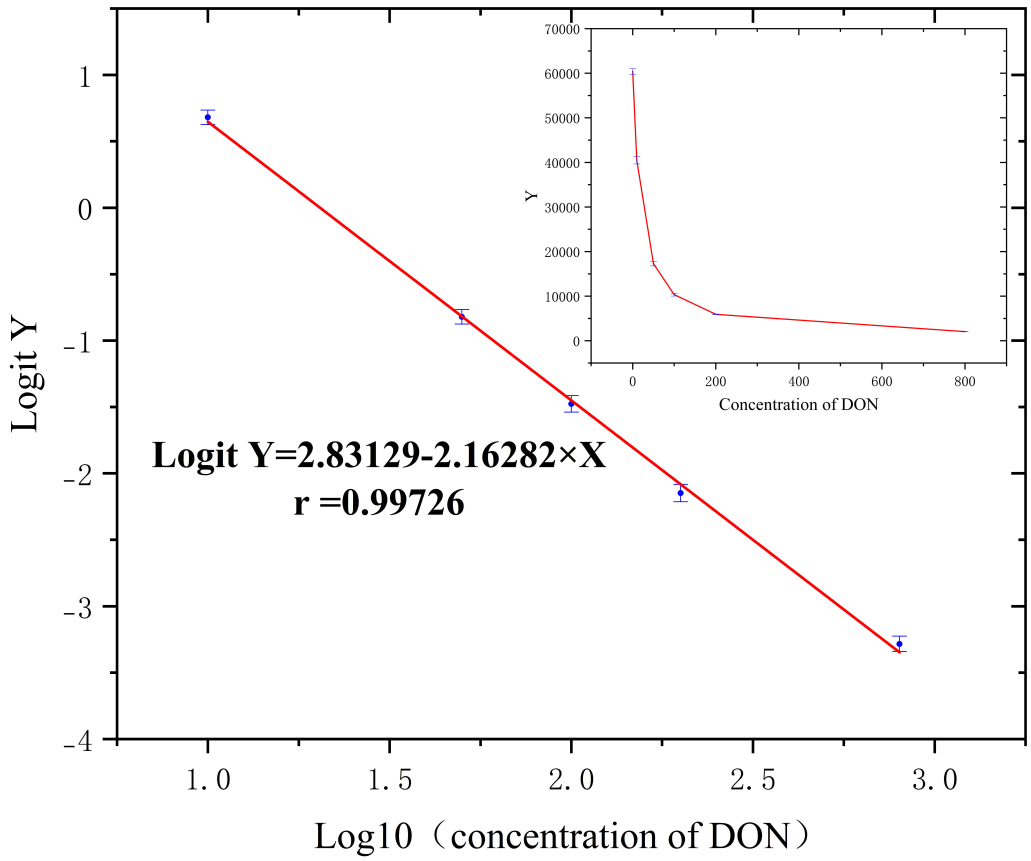

Fig. 3. DON-AlphaLICA standard curve.

Table 1. Precision of DON-AlphaLICA.

Target for testing	Sample concentration to be Measured (ng/mL)	Intra-batch analysis CV (%), n_1 = 10	Batch analysis CV (%), n_2 = 3
DON	10	4.48	3.68
	100	5.44	5.51
	800	6.13	6.67

n_1 = 10: the test sample was tested 10 times; n_2 = 3:3 replicates. DON, Deoxynivalenol; CV, Coefficient of Variation.

Table 2. Recoveries of DON-AlphaLICA spiked samples.

Sample types	Blank concentration (ng/mL)	Standard addition concentration (ng/mL)	Theoretical concentration (ng/mL)	AlphaLICA	
				Mean ± SD (%)	RSD (%)
Wheat	14.97	100	23.47	101.41 ± 2.90	12.17
		200	33.47	91.54 ± 0.78	2.56
		800	93.47	101.23 ± 17.33	18.31
Maize	26.94	100	34.25	101.36 ± 2.58	7.43
		200	44.25	102.84 ± 3.09	6.80
		800	102.59	113.28 ± 17.29	14.88
Rice	0.18	100	10.17	110.15 ± 0.55	4.91
		200	20.17	92.79 ± 3.24	17.31
		800	80.17	89.62 ± 11.70	16.29

SD, standard deviation; RSD, relative standard deviation.

evaluation showed that the recovery rate of 10–800 ng/mL in wheat, corn and rice matrix was 97.52%–105.83% (relative standard deviation (RSD) = 9.70%–12.83%), which met the requirements of AOAC 2006.03 standard (80%–120%) as shown in Table 2. Compared with the traditional ELISA (LOD = 10 ng/mL), the sensitivity of this method was increased by 9.7 times, and the detection period was shortened to 5 min. Its performance parame-

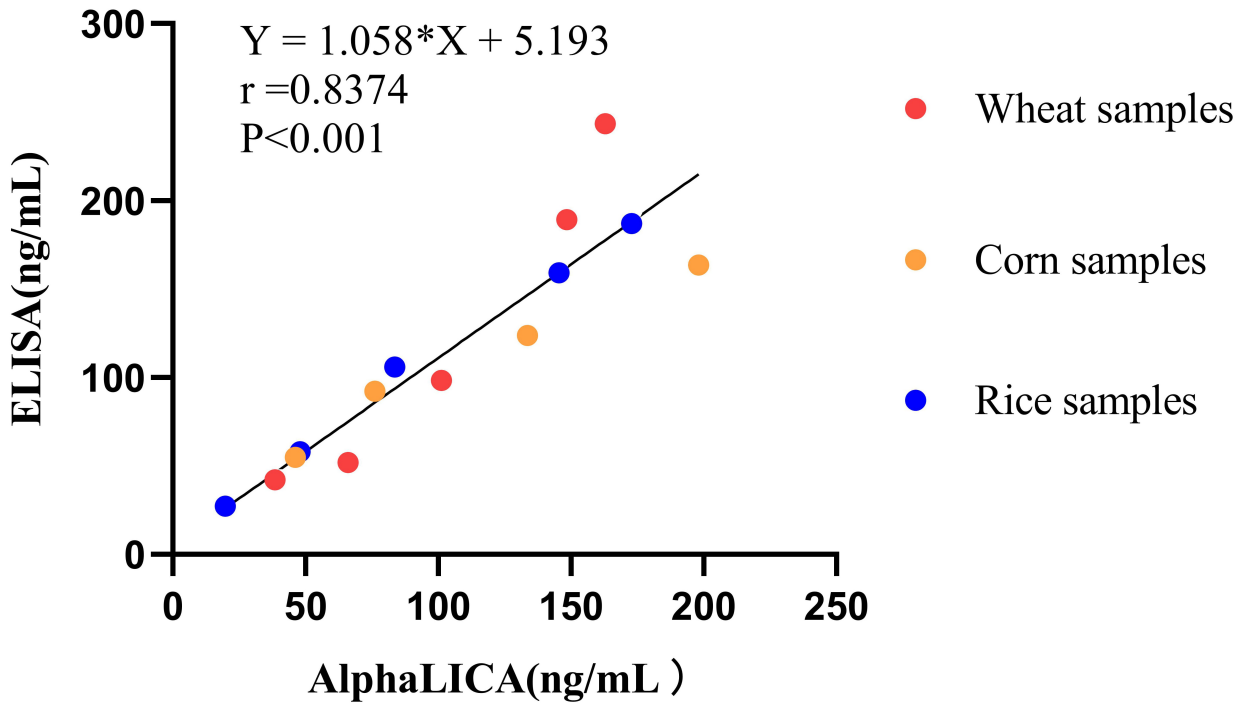

Fig. 4. Comparison of AlphaLICA and enzyme-linked immunosorbent assay (ELISA) results.

ters fully met the detection requirements of DON in grains (LOQ ≤10 ng/mL) in Commission Regulation (EC) No 401 / 2004, which provided a reliable technical solution for on-site monitoring of food security.

3.4 Application of DON-AlphaLICA

In this investigation, the DON-AlphaLICA technique was utilized to quantify DON in authentic wheat, maize, and rice specimens, and the outcomes were benchmarked against ELISA data. The findings are presented in Table 3. A statistically significant positive correlation was observed between the two analytical approaches ($p < 0.001$). The linear regression equation was Y = 1.058X + 5.193 (r = 0.8374), where X and Y represent the detection values of DON-AlphaLICA and ELISA, respectively, as shown in Fig. 4. The empirical findings demonstrated that the DON-AlphaLICA protocol developed in this investigation exhibited strong concordance with the traditional ELISA methodology, and the precise quantification of DON in cereal specimens was effectively accomplished. Through the verification of actual samples, this method shortens the ELISA reaction time from 35 min to 5 min, with higher sensitivity, and the experimental process is free of washing, showing comparability with the existing mature detection technology, which provides a reliable new method for rapid screening of DON pollution in grains.

4. Discussion

DON, a synthesized mycotoxin derived from Fusarium fungi, is ubiquitously distributed in grain cultivars and constitutes a critical hazard to global food security and public health [35,36]. Since its emetic effect was first reported in the 1970s, DON pollution incidents have occurred frequently, especially in wheat, corn and other staple crops in temperate regions. Due to the thermal stability of DON, conventional food processing is difficult to effectively degrade, and it is easy to enter the human dietary chain through contaminated grain products, resulting in acute nausea, vomiting, diarrhea and other symptoms. Long-term low-dose exposure is more likely to cause immunosuppression and intestinal damage [37,38]. The EU stipulates that the limit of DON in wheat and its products is 750 μg/kg, and the Chinese food safety standard sets the limit of DON in cereals to be 1000 μg/kg. In this study, wheat, corn and rice were selected as the detection objects, because they are the main pollution carriers of DON and have a huge circulation. It is of great practical value to establish a fast and accurate DON detection method for food quality monitoring and food safety guarantee.

Based on AlphaLICA technology, this study successfully constructed a highly sensitive and rapid detection system for DON in cereals. The experimental results showed that the method had significant advantages in sensitivity, specificity, repeatability and practicability. The IC_{50} value was 20.47 ng/mL, the LOD was 1.03 ng/mL, the LOQ was 7.57 ng/mL. Traditional immunoassay techniques (such as ELISA) are heterogeneous reaction systems, which require antibodies to coat the microplate and capture the antigen to be tested for detection. The reaction time is long, and the washing step will lead to the dissociation of the antigen-

Table 3. Detection results of the same sample by DON-AlphaLICA and ELISA.

Sample types	Sample number	DON-AlphaLICA results (ng/mL)	ELISA results (ng/mL)
Wheat	1	38.53	42.18
	2	65.99	52.00
	3	101.30	98.24
	4	148.39	189.32
	5	162.95	243.40
Maize	6	46.16	54.83
	7	76.14	92.32
	8	133.71	123.74
	9	198.13	163.65
Rice	10	19.78	27.23
	11	47.94	57.98
	12	83.57	105.91
	13	145.48	159.08
	14	172.81	187.12

antibody complex, resulting in a decrease in the sensitivity of the reaction system [39]. This study is a homogeneous reaction system. Through the design concept of 'no washing', the influence of washing on the detection sensitivity is avoided, and the short-range diffusion characteristics of singlet oxygen are used to realize the construction of space-confined energy transfer network. When the photosensitive microspheres are irradiated with a 680 nm laser, the singlet oxygen generated by the photosensitive microspheres transfers to the luminescent microspheres, and the europium chelate emits 615 nm characteristic fluorescence. Only the complex with the distance between the receptor microspheres and the donor microspheres $<$200 nm can trigger the fluorescence emission of the europium chelate. It is worth noting that the half-life of singlet oxygen is only about 4 µs [40]. This feature not only ensures the instantaneity of signal generation (5 min to complete the detection), but also effectively avoids the interference of oxidizing substances in complex matrices by shortening the energy transfer path.

The recovery rate of wheat, corn and rice samples is stabilized at 97.52%–105.83% (RSD $\leq$12.83%), which is significantly better than the fluctuation caused by the inactivation of nanomaterial sensors due to interface modification [41]. The observed upper limit of RSD was 12.83%, which was close to the maximum threshold of AOAC (15%). The main reason is that the immune detection is greatly affected by time and temperature, and it is difficult to accurately control the reaction time by manual operation. In order to achieve lower RSD and improve the reliability of the actual sample test results, we plan to cooperate with the instrument company to design a fully automatic machine sampling and accurately control the reaction time to achieve millisecond time control (target error $<$0.1 second), which can systematically reduce the interference of human operation.

The DON-AlphaLICA method established in this study has some limitations. First of all, compared with instrumental methods such as liquid chromatography-tandem mass spectrometry (LC-MS/MS), its sensitivity still cannot meet the requirements of trace sample detection, and the quantitative ability of low-polluted grain samples needs to be improved. Secondly, due to the difficulty in obtaining natural contaminated samples, the experimental process is only verified by artificial spiked samples, and the detection data of actual mildewed grain samples need to be supplemented. In future studies, the affinity of antibody-microsphere coupling will be improved to improve the detection sensitivity, and natural contaminated samples of different substrates (wheat, corn, etc.) will be acquired to assess the robustness of the assay. The continuous improvement of this technology will provide more accurate technical support for the rapid screening of grain storage and the monitoring of food processing.

5. Conclusions

In this study, a rapid detection system for DON was constructed based on AlphaLICA technology. Through the energy transfer between microspheres and the principle of specific antigen-antibody binding, efficient and sensitive detection was achieved. This method does not require washing steps, has strong anti-matrix interference ability, significantly shortens the detection time, and the operation process is simple. The reliability and accuracy of the method were verified by experiments, which provided an efficient solution for DON screening in food. In the future, the stability of microspheres will be optimized and practical application scenarios will be expanded to promote the innovative development of mycotoxin detection technology.

Availability of Data and Materials

The data supporting the findings of this study can be obtained from the corresponding authors upon request.

Author Contributions

DL, JC, BH and NHZ designed the research study. DL, BH and SBK performed the research. CLY, TYZ, YQ and XMZ provided help and advice throughout the study. DL, JC, BH and SBK analyzed the data. DL and JC wrote the manuscript. All authors contributed to editorial changes in the manuscript. All authors read and approved the final manuscript. All authors have participated sufficiently in the work and agreed to be accountable for all aspects of the work.

Ethics Approval and Consent to Participate

Not applicable.

Acknowledgment

Not applicable.

Funding

This research was funded by the "Pioneer" and "Leading Goose" R&D Program of Zhejiang (No.2023C03075), Zhejiang Chinese Medical University Affiliated Hospital Research Project (No.2023FSYYZZ22).

Conflict of Interest

The authors declare no conflict of interest.

References

[1] Zingales V, Taroncher M, Martino PA, Ruiz MJ, Caloni F. Climate Change and Effects on Molds and Mycotoxins. Toxins. 2022; 14: 445. https://doi.org/10.3390/toxins14070445.

[2] Liu C, Van der Fels-Klerx HJ. Quantitative Modeling of Climate Change Impacts on Mycotoxins in Cereals: A Review. Toxins. 2021; 13: 276. https://doi.org/10.3390/toxins13040276.

[3] Perrone G, Ferrara M, Medina A, Pascale M, Magan N. Toxigenic Fungi and Mycotoxins in a Climate Change Scenario: Ecology, Genomics, Distribution, Prediction and Prevention of the Risk. Microorganisms. 2020; 8: 1496. https://doi.org/10.3390/microorganisms8101496.

[4] Pinto ACSM, De Pierri CR, Evangelista AG, Gomes ASDLPB, Luciano FB. Deoxynivalenol: Toxicology, Degradation by Bacteria, and Phylogenetic Analysis. Toxins. 2022; 14: 90. https://doi.org/10.3390/toxins14020090.

[5] Hooft JM, Bureau DP. Deoxynivalenol: Mechanisms of action and its effects on various terrestrial and aquatic species. Food and Chemical Toxicology: an International Journal Published for the British Industrial Biological Research Association. 2021; 157: 112616. https://doi.org/10.1016/j.fct.2021.112616.

[6] Ganesan AR, Mohan K, Karthick Rajan D, Pillay AA, Palanisami T, Sathishkumar P, *et al*. Distribution, toxicity, interactive effects, and detection of ochratoxin and deoxynivalenol in food: A review. Food Chemistry. 2022; 378: 131978. https://doi.org/10.1016/j.foodchem.2021.131978.

[7] Lu Q, Luo JY, Ruan HN, Wang CJ, Yang MH. Structure-toxicity relationships, toxicity mechanisms and health risk assessment of food-borne modified deoxynivalenol and zearalenone: A comprehensive review. The Science of the Total Environment. 2022; 806: 151192. https://doi.org/10.1016/j.scitotenv.2021.151192.

[8] Sumarah MW. The Deoxynivalenol Challenge. Journal of Agricultural and Food Chemistry. 2022; 70: 9619–9624. https://doi.org/10.1021/acs.jafc.2c03690.

[9] Kang R, Li R, Dai P, Li Z, Li Y, Li C. Deoxynivalenol induced apoptosis and inflammation of IPEC-J2 cells by promoting ROS production. Environmental Pollution (Barking, Essex: 1987). 2019; 251: 689–698. https://doi.org/10.1016/j.envpol.2019.05.026.

[10] Li E, Horn N, Ajuwon KM. Mechanisms of deoxynivalenol-induced endocytosis and degradation of tight junction proteins in jejunal IPEC-J2 cells involve selective activation of the MAPK pathways. Archives of Toxicology. 2021; 95: 2065–2079. https://doi.org/10.1007/s00204-021-03044-w.

[11] Zhu Z, Wang J, Cheng H, Zhao H, Liu C, Zhou X, *et al*. Combined Toxicity Assessment of Deoxynivalenol and Pb^{2+} on HK-2 Cells Involved in Excessive ROS-Induced Ferroptosis. Journal of Agricultural and Food Chemistry. 2025; 73: 2573–2584. https://doi.org/10.1021/acs.jafc.4c11077.

[12] Songsermsakul P, Razzazi-Fazeli E. A review of recent trends in applications of liquid chromatography-mass spectrometry for determination of mycotoxins. Journal of Liquid Chromatography & Related Technologies. 2008; 31: 1641–1686. https://doi.org/10.1080/10826070802126395.

[13] Abdel-Rahman A, Anyangwe N, Carlacci L, Casper S, Danam RP, Enongene E, *et al*. The safety and regulation of natural products used as foods and food ingredients. Toxicological Sciences: an Official Journal of the Society of Toxicology. 2011; 123: 333–348. https://doi.org/10.1093/toxsci/kfr198.

[14] Pomeranz JL, Broad Leib EM, Mozaffarian D. Regulation of Added Substances in the Food Supply by the Food and Drug Administration Human Foods Program. American Journal of Public Health. 2024; 114: 1061–1070. https://doi.org/10.2105/AJPH.2024.307755.

[15] Righetti L, Galaverna G, Dall'Asta C. Group detection of DON and its modified forms by an ELISA kit. Food Additives & Contaminants. Part A, Chemistry, Analysis, Control, Exposure & Risk Assessment. 2017; 34: 248–254. https://doi.org/10.1080/19440049.2016.1265671.

[16] Sun J, Wang L, Shao J, Yang D, Fu X, Sun X. One-step time-resolved fluorescence microsphere immunochromatographic test strip for quantitative and simultaneous detection of DON and ZEN. Analytical and Bioanalytical Chemistry. 2021; 413: 6489–6502. https://doi.org/10.1007/s00216-021-03612-0.

[17] Russ M, Hauser S, Wintersteiger R, Greilberger J, Andrä M, Ortner A. Determination of Angiotensin-(1-7) with HPLC/Fluorescence-Detection. Journal of Fluorescence. 2016; 26: 81–86. https://doi.org/10.1007/s10895-015-1686-y.

[18] You F, Wen Z, Yuan R, Qian J, Long L, Wang K. Sensitive and stable detection of deoxynivalenol based on electrochemiluminescence aptasensor enhanced by 0D/2D homojunction effect in food analysis. Food Chemistry. 2023; 403: 134397. https://doi.org/10.1016/j.foodchem.2022.134397.

[19] Luo S, Liu Y, Guo Q, Wang X, Tian Y, Yang W, *et al*. Determination of Zearalenone and Its Derivatives in Feed by Gas Chromatography-Mass Spectrometry with Immunoaffinity Column Cleanup and Isotope Dilution. Toxins. 2022; 14: 764. https://doi.org/10.3390/toxins14110764.

[20] Romero-Sánchez I, Ramírez-García L, Gracia-Lor E, Madrid-Albarrán Y. Simultaneous determination of aflatoxins B1, B2, G1 and G2 in commercial rices using immunoaffinity column clean-up and HPLC-MS/MS. Food Chemistry. 2022; 395: 133611. https://doi.org/10.1016/j.foodchem.2022.133611.

[21] Ji F, Li H, Xu J, Shi J. Enzyme-linked immunosorbent-assay for Deoxynivalenol (DON). Toxins. 2011; 3: 968–978. https://doi.org/10.3390/toxins3080968.

[22] Maragos CM. Signal amplification using colloidal gold in a biolayer interferometry-based immunosensor for the mycotoxin deoxynivalenol. Food Additives & Contaminants. Part A, Chemistry, Analysis, Control, Exposure & Risk Assessment.

2012; 29: 1108–1117. https://doi.org/10.1080/19440049.2012.671789.

[23] Kolosova AY, Sibanda L, Dumoulin F, Lewis J, Duveiller E, Van Peteghem C, *et al*. Lateral-flow colloidal gold-based immunoassay for the rapid detection of deoxynivalenol with two indicator ranges. Analytica Chimica Acta. 2008; 616: 235–244. https://doi.org/10.1016/j.aca.2008.04.029.

[24] Kolosova AY, De Saeger S, Sibanda L, Verheijen R, Van Peteghem C. Development of a colloidal gold-based lateral-flow immunoassay for the rapid simultaneous detection of zearalenone and deoxynivalenol. Analytical and Bioanalytical Chemistry. 2007; 389: 2103–2107. https://doi.org/10.1007/s00216-007-1642-z.

[25] Xiao X, Zhou Q, Zhu J, Sun L, Zhang H, Sun Y, *et al*. False-positive colloidal gold-based immunochromatographic strip assay reactions for antibodies to SARS-CoV-2 in patients with autoimmune diseases. Annals of Translational Medicine. 2021; 9: 534. https://doi.org/10.21037/atm-20-6509.

[26] Zhang J, Xu J, Shen S, Ding L, Yang W, Tang C, *et al*. Comparison of three colloidal gold immunoassays and GeneXpert Carba-R for the detection of *Klebsiella pneumoniae bla*$_{KPC-2}$ variants. Journal of Clinical Microbiology. 2024; 62: e0015424. https://doi.org/10.1128/jcm.00154-24.

[27] Wang Y, Wang T, Wang M, Wang J, Xu Z, Zhang H. Photothermal card reader assay using the commercial colloidal gold test strip for the rapid quantitative detection of food hazards. Mikrochimica Acta. 2022; 189: 112. https://doi.org/10.1007/s00604-022-05193-w.

[28] Jin Y, He Y, Zhao D, Chen Y, Xue Q, Zou M, *et al*. Development of an amplified luminescent proximity homogeneous assay for the detection of sulfonamides in animal-derived products. Food Science & Nutrition. 2021; 9: 4938–4945. https://doi.org/10.1002/fsn3.2443.

[29] Qin Y, Li J, Kuang J, Shen S, Zhou X, Zhao X, *et al*. Okadaic Acid Detection through a Rapid and Sensitive Amplified Luminescent Proximity Homogeneous Assay. Toxins. 2023; 15: 501. https://doi.org/10.3390/toxins15080501.

[30] Zhao C, Zhang Z, Li J, Lu Y, Ma F, Wang Z, *et al*. Development of a Quick and Highly Sensitive Amplified Luminescent Proximity Homogeneous Assay for Detection of Saxitoxin in Shellfish. Toxins. 2024; 16: 341. https://doi.org/10.3390/toxins16080341.

[31] Monaghan TF, Rahman SN, Agudelo CW, Wein AJ, Lazar JM, Everaert K, *et al*. Foundational Statistical Principles in Medical Research: Sensitivity, Specificity, Positive Predictive Value, and Negative Predictive Value. Medicina (Kaunas, Lithuania). 2021; 57: 503. https://doi.org/10.3390/medicina57050503.

[32] Liu EY, Jung S, Yi H. Improved Protein Conjugation with Uniform, Macroporous Poly(acrylamide-co-acrylic acid) Hydrogel Microspheres via EDC/NHS Chemistry. Langmuir: the ACS Journal of Surfaces and Colloids. 2016; 32: 11043–11054. https://doi.org/10.1021/acs.langmuir.6b02591.

[33] Wright TA, Rahman MS, Bennett C, Johnson MR, Fischesser H, Ram N, *et al*. Hydrolytically Stable Maleimide-End-Functionalized Polymers for Site-Specific Protein Conjugation. Bioconjugate Chemistry. 2021; 32: 2447–2456. https://doi.org/10.1021/acs.bioconjchem.1c00487.

[34] Zhuang SH, Guo XX, Wu YS, Chen ZH, Chen Y, Ren ZQ, *et al*. Quantum Dot-Based Luminescent Oxygen Channeling Assay for Potential Application in Homogeneous Bioassays. Journal of Fluorescence. 2016; 26: 317–322. https://doi.org/10.1007/s10895-015-1716-9.

[35] O'Mara SP, Broz K, Boenisch M, Zhong Z, Dong Y, Kistler HC. The *Fusarium graminearum* t-SNARE *Sso2* Is Involved in Growth, Defense, and DON Accumulation and Virulence. Molecular Plant-microbe Interactions: MPMI. 2020; 33: 888–901. https://doi.org/10.1094/MPMI-01-20-0012-R.

[36] Abbas A, Yli-Mattila T. Biocontrol of *Fusarium graminearum*, a Causal Agent of Fusarium Head Blight of Wheat, and Deoxynivalenol Accumulation: From *In Vitro* to *In Planta*. Toxins. 2022; 14: 299. https://doi.org/10.3390/toxins14050299.

[37] Wu Q, Kuča K, Humpf HU, Klímová B, Cramer B. Fate of deoxynivalenol and deoxynivalenol-3-glucoside during cereal-based thermal food processing: a review study. Mycotoxin Research. 2017; 33: 79–91. https://doi.org/10.1007/s12550-016-0263-9.

[38] Awad WA, Aschenbach JR, Zentek J. Cytotoxicity and metabolic stress induced by deoxynivalenol in the porcine intestinal IPEC-J2 cell line. Journal of Animal Physiology and Animal Nutrition. 2012; 96: 709–716. https://doi.org/10.1111/j.1439-0396.2011.01199.x.

[39] Hunt JH, Jones JL, Gebo KA, Hansoti B, Traut CC, Hamill MM, *et al*. Discordant performance of mpox serological assays. Journal of Virological Methods. 2024; 329: 115004. https://doi.org/10.1016/j.jviromet.2024.115004.

[40] Partanen SB, Apell JN, Lin J, McNeill K. Factors affecting the mixed-layer concentrations of singlet oxygen in sunlit lakes. Environmental Science. Processes & Impacts. 2021; 23: 1130–1145. https://doi.org/10.1039/d1em00062d.

[41] Hassan MM, Xu Y, Zareef M, Li H, Rong Y, Chen Q. Recent advances of nanomaterial-based optical sensor for the detection of benzimidazole fungicides in food: a review. Critical Reviews in Food Science and Nutrition. 2023; 63: 2851–2872. https://doi.org/10.1080/10408398.2021.1980765.